

## Nucleon Momentum Distributions and Elastic Electron Scattering form Factors for $^{54}\text{Fe}$ , $^{56}\text{Fe}$ and $^{58}\text{Fe}$ Isotopes

Ahmed N. Abdullah

Department of Physics, College of Science, University of Baghdad, Baghdad-Iraq.

E-mail: Ahmednajim1979@yahoo.com.

### Abstract

The nucleon momentum distributions and elastic electron scattering form factors of the ground state for some  $1f-2p$  shell nuclei, such as  $^{54}\text{Fe}$ ,  $^{56}\text{Fe}$  and  $^{58}\text{Fe}$  isotopes, have been studied utilizing the Coherent Density Fluctuation Model formulated by means of the fluctuation function (weight function). The fluctuation function has been connected to the nucleon density distribution of the nuclei and obtained from the theory and experiment. The feature of the long-tail behavior at high momentum region of the nucleon momentum distributions has been determined by both the theoretical and experimental fluctuation functions. The calculated elastic electron scattering form factors for considered isotopes are in a good agreement with those of experimental data throughout all values of momentum transfer  $q$ .

Keywords: Nucleon density distributions, Nucleon momentum distributions, Coherent density fluctuation model.

### Introduction

There is no method for directly measuring the nucleon momentum distribution (NMD) in nuclei. The quantities that are measured by particle-nucleus and nucleus-nucleus collisions are the cross sections of different reactions, and these contain information on the (NMD) of target nucleons. The experimental evidence obtained from inclusive and exclusive electron scattering on nuclei establish the existence of long-tail behavior of the (NMD) at high momentum region ( $k \geq 2 \text{ fm}^{-1}$ ) [1,2]. In principle, mean field theories cannot describe correctly the form factors  $F(q)$  and the (NMD) simultaneously [3] and they exhibit a steep-slope behavior of the (NMD) at high momentum region. In fact, the (NMD) depends a little on the effective mean field considered due to its sensitivity to the short-range and tensor nucleon-nucleon correlations [3, 4] which are not included in the mean field theories. There are several theoretical methods used to study elastic electron-nucleus scattering, such as the plan-wave Born approximation (PWBA), the eikonal approximation and the phase-shift analysis method [5-8].

In coherent density fluctuations model (CDFM), which is exemplified by the work of Antonov *et al.* [9,10,11], the local nucleon density distribution (NDD) and the nucleon

momentum distributions (NMD) are simply related and expressed in terms of experimentally obtainable fluctuation function (weight function)  $|f(x)|^2$ . They [9,10,11] studied the NMD of ( $^4\text{He}$  and  $^{16}\text{O}$ ),  $^{12}\text{C}$  and ( $^{39}\text{K}$ ,  $^{40}\text{Ca}$  and  $^{48}\text{Ca}$ ) nuclei using weight functions  $|f(x)|^2$  specified by the two parameter Fermi (2PF) NDD [12], the data of Reuter *et al.* [13] and the model independent NDD [12], respectively. It is significant to remark that all above studies, employing the framework of the CDFM, proved a high momentum tail in the NMD. Elastic electron scattering from  $^{40}\text{Ca}$  nucleus was also investigated in Ref. [9], where the calculated elastic differential cross sections ( $d\sigma/d\Omega$ ) are in good agreement with those of experimental data.

In the present study, we utilize the CDFM with weight functions originating in terms of theoretical NDD. We first try to derive a theoretical form for the NDD, applicable throughout all  $fp$ -shell nuclei, based on the use of the single particle harmonic oscillator wave function and the occupation numbers of the states. The derived form of the NDD is employed in determining the theoretical weight function  $|f(x)|^2$  which is then used in the CDFM to study the nucleon momentum distribution (NMD) and elastic form factors for  $^{54}\text{Fe}$ ,  $^{56}\text{Fe}$  and  $^{58}\text{Fe}$  isotopes. It is found that

the theoretical weight function  $|f(x)|^2$  based on the derived NDD is capable to give information about the NMD and elastic charge form factors as do those of the experimental data.

**Theory**

The nucleon density distribution NDD of one body operator can be written as [14,15]:

$$\rho(r) = \frac{1}{4\pi} \sum_{n\ell} \xi_{n\ell} 4(2\ell + 1) |R_{n\ell}|^2 \dots\dots\dots (1)$$

where  $\xi_{n\ell}$  is the nucleon occupation probability of the state  $n\ell$  ( $\xi_{n\ell} = 0$  or  $1$  for closed shell nuclei and  $0 < \xi_{n\ell} < 1$  for open shell nuclei) and  $R_{n\ell}$  is the radial part of the single particle harmonic oscillator wave function.

$$\rho(r) = \frac{e^{-r^2/b^2}}{\pi^{3/2} b^3} \left\{ 10 - \frac{3}{2} \alpha_1 + \left( \frac{11}{3} \alpha_1 + \frac{5}{3} \alpha_2 \right) \left( \frac{r}{b} \right)^2 + \left( 8 - 2\alpha_1 - \frac{4}{3} \alpha_2 \right) \left( \frac{r}{b} \right)^4 + \left( \frac{20}{105} \alpha_2 + \frac{8}{105} (A - 40) + \frac{4}{15} \alpha_1 \right) \left( \frac{r}{b} \right)^6 \right\} \dots\dots\dots (2)$$

where  $A$  is the nuclear mass number,  $b$  is the harmonic oscillator size parameter. The parameter  $\alpha_1$  characterizes the deviation of the nucleon occupation numbers from the prediction of the simple shell model ( $\alpha_1 = 0$ ). The parameter  $\alpha_2$  in Eq. (2) is assumed as a free parameter to be adjusted to obtain agreement with the experimental NDD.

The normalization condition of the  $\rho(r)$  is given by

$$A = 4\pi \int_0^\infty \rho(r) r^2 dr \dots\dots\dots (3)$$

and the mean square radius (MSR) of the considered nuclei is given by

$$\langle r^2 \rangle = \frac{4\pi}{A} \int_0^\infty \rho(r) r^4 dr \dots\dots\dots (4)$$

The central NDD,  $\rho(r = 0)$  is obtained from Eq. (2) as

$$\rho(0) = \frac{1}{\pi^{3/2} b^3} \left[ 10 - \frac{3}{2} \alpha_1 \right] \dots\dots\dots (5)$$

then  $\alpha_1$  is obtained from Eq. (5) as

$$\alpha_1 = \frac{2}{3} (10 - \rho(0) \pi^{3/2} b^3) \dots\dots\dots (6)$$

Substituting Eq. (2) into Eq. (4) and after simplification gives:

The NDD form of *Fe*-isotopes is derived on the assumption that there are filled 1s, 1p and 1d orbitals and the nucleon occupation numbers in 2s, 1f and 2p orbitals are equal to, respectively,  $(4 - \alpha_1)$ ,  $(A - 40 - \alpha_2)$  and  $(\alpha_1 + \alpha_2)$  and not to 4,  $(A-40)$  and 0 as in the simple shell model. Using this assumption in Eq. (1), an analytical form for the ground state NDD of *Fe*-isotopes is obtained as:

$$\langle r^2 \rangle = \frac{b^2}{A} \left[ \frac{9A-120}{2} + \alpha_1 \right] \dots\dots\dots (7)$$

In Eq's (5) and (7), the values of the central density  $\rho(0)$  and  $\langle r^2 \rangle$  are taken from the experiments while the parameter  $b$  is chosen in such a way as to reproduce the experimental root mean square radii of nuclei.

The NMD of the considered nuclei is studied using two distinct methods. In the first, it is determined by the shell model using the single particle harmonic oscillator wave functions in momentum representation and is given by [16]:

$$n(k) = \frac{b^3}{\pi^{3/2}} e^{-b^2 k^2} \left[ 10 + 8 (bk)^4 + \frac{8(A-40)}{105} (bk)^6 \right] \dots\dots\dots (8)$$

where  $k$  is the momentum of the particle.

In the second method, the NMD is determined by the Coherent Density Fluctuation Model (CDFM), where the mixed density is given by [9, 10]

$$\rho(r, r') = \int_0^\infty |f(x)|^2 \rho_x(r, r') dx \dots\dots\dots (9)$$

where:

$$\rho_x(r, r') = 3\rho_0(x) \frac{j_1(k_F(x)|\bar{r} - \bar{r}'|)}{k_F(x)|\bar{r} - \bar{r}'|} \theta(\bar{x} - \frac{1}{2}|\bar{r} + \bar{r}'|) \dots\dots\dots (10)$$

is the density matrix for  $A$  nucleons uniformly distributed in a sphere with radius  $x$  and density  $\rho_0(x) = 3A/4\pi x^3$ . The Fermi momentum is defined as [9, 10]:

$$k_F(x) = \left( \frac{3\pi^2}{2} \rho_0(x) \right)^{1/3} \equiv \frac{V}{x} \dots\dots\dots (11)$$

and the step function  $\theta$ , is defined by

$$\theta(y) = \begin{cases} 1, & y \geq 0 \\ 0, & y < 0 \end{cases} \dots\dots\dots (12)$$

The diagonal element of Eq. (9) gives the one-particle density as

$$\rho(r) = \rho(r, r') \Big|_{r=r'} = \int_0^\infty |f(x)|^2 \rho_x(r) dx \dots\dots\dots (13)$$

In eq. (13),  $\rho_x(r)$  and  $|f(x)|^2$  have the following forms [9, 10]:

$$\rho_x(r) = \rho_0(x)\theta(x-r) \dots\dots\dots (14)$$

$$|f(x)|^2 = \frac{-1}{\rho_0(x)} \frac{d\rho(r)}{dr} \Big|_{r=x} \dots\dots\dots (15)$$

The weight function of Eq. (15), determined in terms of the NDD satisfies the following normalization condition [9, 10]

$$\int_0^\infty |f(x)|^2 dx = 1, \dots\dots\dots (16)$$

and holds for monotonically decreasing density NDD distribution, i.e.  $\frac{d\rho(r)}{dr} < 0$ .

On the basis of eq. (13), the NMD  $[n(k)]$  is expressed as [9, 10]:

$$n(k) = \int_0^\infty |f(x)|^2 n_x(k) dx, \dots\dots\dots (17)$$

Where

$$n_x(k) = \frac{4}{3} \pi x^3 \theta(k_F(x) - |\vec{k}|), \dots\dots\dots (18)$$

is the Fermi-momentum distribution of the system with density  $\rho_0(x)$ . By means of Eqs. (15), (17) and (18), an explicit form for the NMD is expressed in terms of  $\rho(r)$  as

$$n_{CDFM}(k) = \left( \frac{4\pi}{3} \right)^2 \frac{4}{A} \int_0^{V/k} \left[ 6\rho(x)x^5 dx - \left( \frac{V}{k} \right)^6 \rho \left( \frac{V}{k} \right) \right] \dots\dots\dots (19)$$

with normalization condition

$$A = \int n_{CDFM}(k) \frac{d^3k}{(2\pi)^3} \dots\dots\dots (20)$$

The elastic monopole form factor  $F(q)$  of the target nucleus is also expressed in the CDFM as [9, 10]:

$$F(q) = \frac{1}{A} \int_0^\infty |f(x)|^2 F(q, x) dx \dots\dots\dots (21)$$

where  $F(q, x)$  is the form factor of uniform charge density distribution given by:

$$F(q, x) = \frac{3A}{(qx)^2} \left[ \frac{\sin(qx)}{(qx)} - \cos(qx) \right] \dots\dots\dots (22)$$

Inclusion of the corrections of the nucleon finite size  $F_{fs}(q)$  and the center of mass corrections  $F_{cm}(q)$  in the calculations requires multiplying the form factor of equation (22) by these corrections. Here,  $F_{fs}(q)$  is considered as free nucleon form factor which is assumed to be the same for protons and neutrons. This correction takes the form [17]:

$$F_{fs}(q) = e^{\left( \frac{-0.43q^2}{4} \right)} \dots\dots\dots (23)$$

The correction  $F_{cm}(q)$  removes the spurious state arising from the motion of the center of mass when shell model wave function is used and given by [17]:

$$F_{cm}(q) = e^{\left( \frac{b^2 q^2}{4A} \right)} \dots\dots\dots (24)$$

It is important to point out that all physical quantities studied above in the framework of the CDFM such as NMD and  $F(q)$ , are expressed in terms of the weight function  $|f(x)|^2$ . Therefore, it is worthwhile trying to obtain the weight function firstly from the NDD of two-parameter Fermi (2PF) model extracted from the analysis of elastic electron-nuclei scattering experiments and secondly

from theoretical considerations. The NDD of 2PF is given by [12]

$$\rho(r) = \rho_0 / (1 + \exp(r - c)/z) \dots\dots\dots (25)$$

Introducing Eq. (25) into Eq. (15), we obtain the experimental weight function  $|f(x)|_{2PF}^2$  as

$$|f(x)|_{2PF}^2 = \frac{4\pi x^3 \rho_0}{3Az} \left( 1 + e^{\frac{x-c}{z}} \right)^{-2} \exp\left(\frac{x-c}{z}\right) \dots\dots\dots (26)$$

Moreover, introducing the derived NDD of Eq. (2) into Eq. (15), we obtain the theoretical weight function  $|f(x)|^2$  as

$$|f(x)|_{th}^2 = \frac{8\pi x^4}{3Ab^2} \rho(x) - \frac{16x^4}{3A\pi^{1/2}b^5} \left\{ \frac{11}{6} \alpha_1 + \frac{5}{6} \alpha_2 + \left( 8 - 2\alpha_1 - \frac{4}{3} \alpha_2 \right) \left( \frac{x}{b} \right)^2 + \left( \frac{4}{35} (A - 40) + \frac{2}{5} \alpha_1 + \frac{2}{7} \alpha_2 \right) \left( \frac{x}{b} \right)^4 \right\} e^{-x^2/b^2} \dots\dots\dots (27)$$

**Results and Discussion**

The nucleon momentum distribution  $n(k)$  and elastic electron scattering form factors for <sup>54</sup>Fe, <sup>56</sup>Fe and <sup>58</sup>Fe isotopes are studied by means of the CDFM. The distribution  $n(k)$  of Eq. (19) is calculated in terms of the NDD

obtained firstly from theoretical consideration as in Eq. (2) and secondly from experiments, such as, 2PF [12]. The harmonic oscillator size parameter  $b$  is chosen such that to reproduce the measured root mean square radii (*rms*) of nuclei under study and the parameter  $\alpha_1$  is determined by introducing the chosen value of  $b$  and the experimental central density  $\rho_{exp}(0)$  into Eq. (6), while the parameter  $\alpha_2$  is assumed as a free parameter to be adjusted to obtain agreement with the experimental *NDD*. It is important to remark that when  $\alpha_1 = \alpha_2 = 0$ , Eq.(2) is reduced to that of the simple shell model prediction. The values of the parameters  $b$  and  $\alpha_1$  together with the other parameters employed in the present calculations for isotopes under study are listed in Table (1). The calculated rms  $\langle r^2 \rangle_{cal}^{1/2}$  and those of experimental data  $\langle r^2 \rangle_{exp}^{1/2}$  [12] are displayed in this table as well for comparison. The comparison shows a remarkable agreement between  $\langle r^2 \rangle_{cal}^{1/2}$  and  $\langle r^2 \rangle_{exp}^{1/2}$  for all considered isotopes. The calculated occupation numbers of nucleons in the orbitals 2s, 1f and 2p, which are equal to  $(4 - \alpha_1)$ ,  $(A - 40 - \alpha_2)$  and  $(\alpha_1 + \alpha_2)$  respectively, of the considered isotopes are displayed in Table (2).

**Table (1)**

*Parameters for the NDD of considered isotopes together with  $\langle r^2 \rangle_{cal}^{1/2}$  and  $\langle r^2 \rangle_{exp}^{1/2}$ .*

Nucleus	2PF [12]		$\rho_{exp}(0) fm^{-3}$ [12]	$\langle r^2 \rangle_{cal}^{1/2}$	$\langle r^2 \rangle_{exp}^{1/2}$ [12]	$b$	$\alpha_1$	$\alpha_2$
	$c$	$z$						
<sup>54</sup> Fe	4.075	0.506	0.16524	3.733	3.732	2.019	1.6149	1.0142
<sup>56</sup> Fe	4.111	0.558	0.16269	3.801	3.801	2.045	1.4983	1.3978
<sup>58</sup> Fe	4.027	0.576	0.17623	3.873	3.873	2.026	1.2227	2.2989

**Table (2)**

*Calculated occupation numbers of 2s, 1f and 2p orbitals of the considered isotopes.*

Nucleus	Occupation No. of 2s $(4 - \alpha_1)$	Occupation No. of 1f $(A - 40 - \alpha_2)$	Occupation No. of 2p $(\alpha_1 + \alpha_2)$
<sup>54</sup> Fe	2.3850	12.9858	2.6291
<sup>56</sup> Fe	2.5016	14.6022	2.8961
<sup>58</sup> Fe	2.7772	15.6011	3.6216

The dependence of the NDD's (in  $\text{fm}^{-3}$ ) on  $r$  (in fm) for  $^{54}\text{Fe}$ ,  $^{56}\text{Fe}$  and  $^{58}\text{Fe}$  isotopes is shown in Fig.(1). The blue and red curves are the calculated results using Eq. (2) with  $\alpha_1 = \alpha_2 = 0$  and  $\alpha_1 \neq \alpha_2 \neq 0$ , respectively whereas the filled circle symbols correspond to the experimental data [12]. It is obvious that the form of the CDD represented by Eq. (2) behaves as an exponentially decreasing function, as seen by the red and blue curves for all considered nuclei of Fig.(1). This figure shows that the probability of finding a proton near the central region ( $0 \leq r \leq 2$  fm) of the CDD is larger than the tail region ( $r > 2$  fm). Besides, including the higher shells through introducing the values of  $\alpha_1$  and  $\alpha_2$  [presented in Table (1)] into Eq. (3) leads to decreasing significantly the central region of the CDD and increasing slightly the tail region of the CDD, as seen by the red curves. This means that the effect of inclusion of higher shells tends to increase the probability of transferring the protons from the central region of the nucleus towards its surface region and then makes the nucleus to be less rigid than the case when there is no this effect. Fig.(1) also illustrates that the blue curves in all considered nuclei are not in good agreement with those of experimental data of Ref.[12], especially at the central region of the CDD. But once the higher shells are considered to the calculations, the calculated results for the CDD become in astonishing agreement with those of experimental data throughout the whole range of  $r$  as seen by the red curves.

The dependence of NMD (in  $\text{fm}^3$ ) on  $k$  (in  $\text{fm}^{-1}$ ) for  $^{54}\text{Fe}$ ,  $^{56}\text{Fe}$  and  $^{58}\text{Fe}$  isotopes is shown in Fig.(2). The blue curves are the calculated NMD of Eq.(8) obtained by the shell model calculation using the single particle harmonic oscillator wave functions in momentum representation. The filled circle symbols and red curves are the NMD obtained by the CDFM of Eq. (19) using the experimental and theoretical NDD, respectively. It is clear that the behavior of the blue curves obtained by the shell model calculations is in contrast with those reproduced by the CDFM. The important feature of the blue distributions is the steep slope behavior when  $k$  increases. This behavior is in disagreement with the studies

[9,10,18-20] and it is attributed to the fact that the ground state shell model wave function given in terms of a Slater determinant does not take into account the important effect of the short range dynamical correlation functions. Hence, the short-range repulsive features of the nucleon-nucleon forces are responsible for the high momentum behavior of the NMD [18,19]. It is noted that the general structure of the filled circle symbols and red curves at the region of high momentum components is almost the same for  $^{54}\text{Fe}$ ,  $^{56}\text{Fe}$  and  $^{58}\text{Fe}$  isotopes, where these curves have the property of long tail manner at momentum region  $k \geq 2 \text{ fm}^{-1}$ . The property of long-tail manner obtained by the CDFM, which is in agreement with the studies [9, 10, 18- 20], is connected to the presence of high densities  $\rho_x(r)$  in the decomposition of Eq. (14), though their fluctuation functions  $|f(x)|^2$  are small.

The dependence of elastic electron scattering form factors,  $F(q)$ , on the momentum transfer  $q$  (in  $\text{fm}^{-1}$ ) for considered isotopes is shown in Fig.(3). As there is no data available for  $^{54}\text{Fe}$ ,  $^{56}\text{Fe}$  and  $^{58}\text{Fe}$  isotopes we have compared the calculated form factors (red curves) of these isotopes obtained in the framework of CDFM using the theoretical weight function of Eq. (27), with those obtained by the Fourier transform of the 2PF density (filled circle symbols) [12]. This figure shows that the red curves are in very good agreement with those fitted to the experimental data up to momentum transfer  $q \approx 1.8 \text{ fm}^{-1}$ , whereas for  $q > 1.8 \text{ fm}^{-1}$  the calculated form factors underestimate those fitted to experimental data. All the first and second diffraction minima are reproduced in the correct places.

## Conclusion

It is concluded that the derived form of NDD of Eq.(2) employed in the determination of theoretical weight function of Eq. (27) is capable to reproduce information about the NMD and elastic form factors as do those of the experimental data.

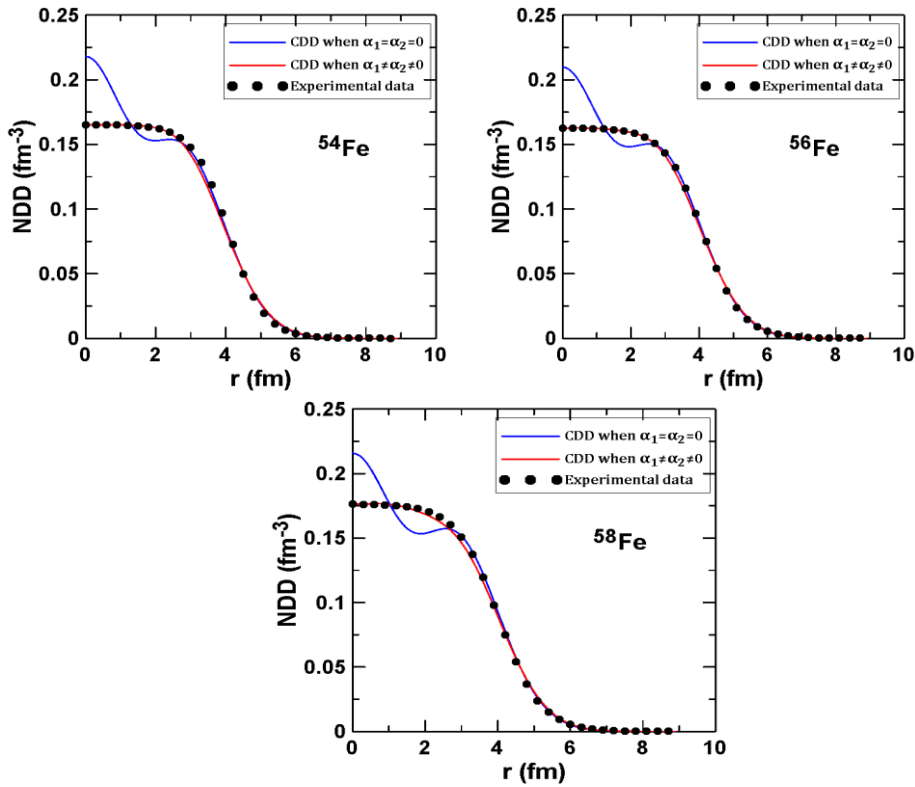


Fig.(1): The dependence of the NDD on  $r$  for  $^{54}\text{Fe}$ ,  $^{56}\text{Fe}$  and  $^{58}\text{Fe}$  isotopes. The blue and red curves are the calculated NDD of Eq. (2) when  $\alpha_1 = \alpha_2 = 0$  and  $\alpha_1 \neq \alpha_2 \neq 0$ , respectively. The filled circle symbols are the experimental data taken from ref. [12].

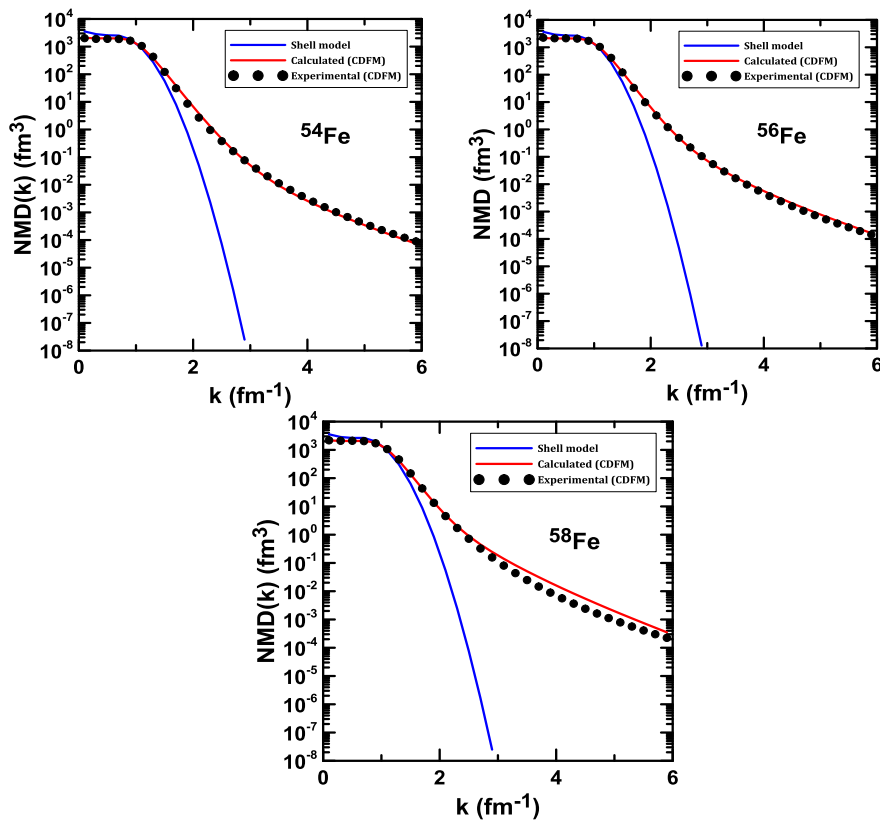
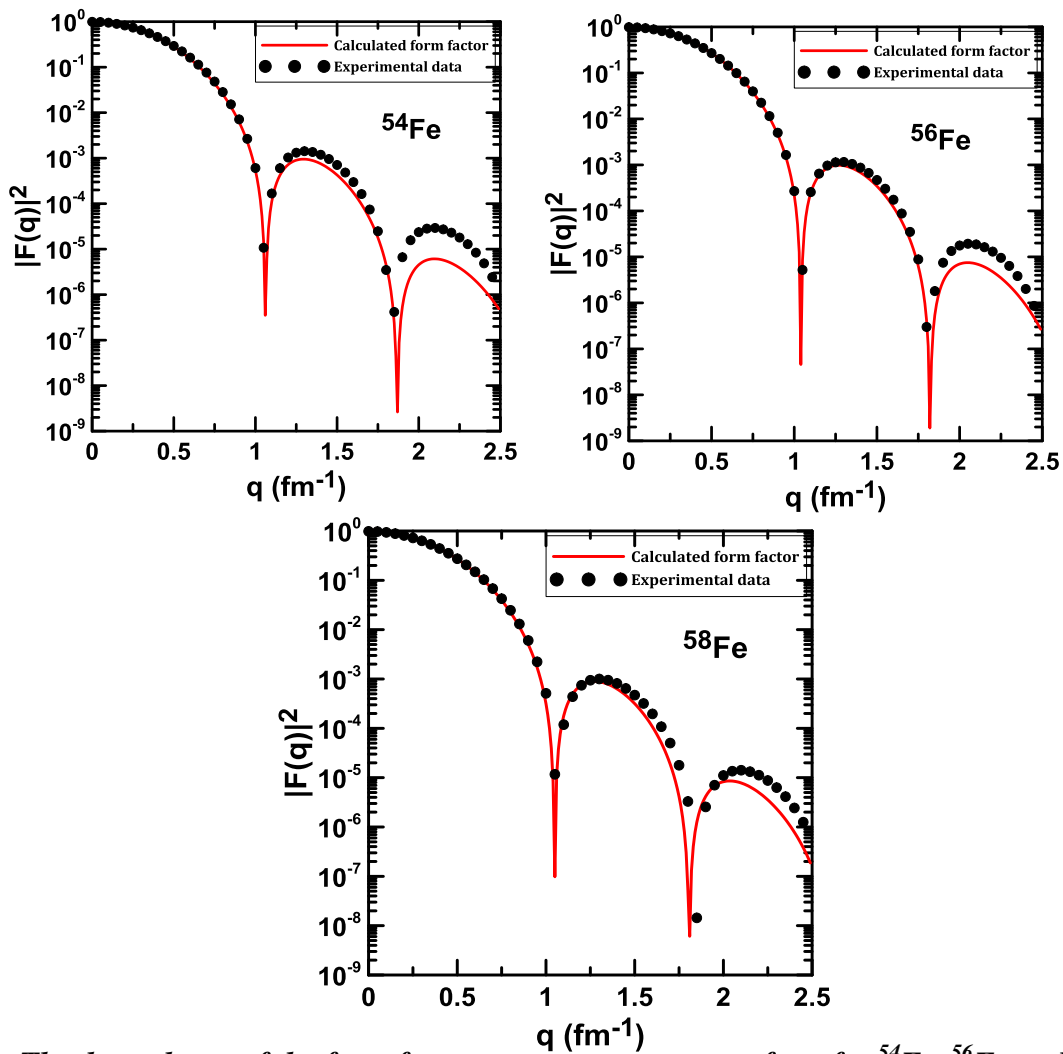


Fig.(2): The dependence of NMD on  $k$  for  $^{54}\text{Fe}$ ,  $^{56}\text{Fe}$  and  $^{58}\text{Fe}$  isotopes. The red curves and filled circle symbols are the calculated NMD expressed by the CDFM of Eq. (19) using the theoretical NDD of Eq. (2) and the experimental data of ref. [12], respectively. The blue curves are the calculated NMD of Eq. (8) obtained by the shell model calculation using the single-particle harmonic oscillator wave functions in momentum representation.



**Fig.(3):** The dependence of the form factors on momentum transfer  $q$  for  $^{54}\text{Fe}$ ,  $^{56}\text{Fe}$  and  $^{58}\text{Fe}$  isotopes. The red curves are the form factors calculated using Eq. (21). The filled circle symbols are the form factors obtained by the Fourier transform of the (2PF) [12].

## References

- [1] Amado R. D., and Woloshyn R. M., "Mechanism for  $180^\circ$  proton production in energetic proton-nucleus collisions", Phys. Rev. Lett., 36, 1435, 1976.
- [2] Komarov V. I., Kosarey G. E., H. Muler, Netzband D. and Stiehler T., "Inclusive spectra and the angular distribution of protons emitted backwards in the interaction of 640 MeV protons with nuclei", Phys. Lett., B 69, 37, 1977.
- [3] Traini M. and Orlandini V., "Nucleon momentum distributions in doubly closed shell nuclei", Z.Physik, A321, 479, 1985.
- [4] Dal Ri M., Stringari S. and Bohigas O., "Effects of short range correlations on one- and two-body properties of nuclei", Nucl. Phys., A 376, 81, 1982.
- [5] Wang Z. and Ren Z., "systematic study of charge form factors of elastic electron-nucleus scattering with relativistic eikonal approximation", Phys. Rev., C 71, 5432\_1-54323\_9, 2005.
- [6] Wang Z. and Ren Z. and fan Y., "Charge density distributions and charge form factors of the N=82 and N=126 isotonic nuclei", Phys. Rev., C 73, 14610\_1-14610\_9, 2006.
- [7] Roca-Maza X., Centelles M., Salvat F. and Vinas X., "Theoretical study of the elastic electron scattering off stable and exotic nuclei", Phys. Rev., C 78, 44332\_1-44332\_16, 2008.
- [8] Chu Y., Ren Z., Dong T. and Wang Z., "Theoretical study of nuclear charge densities with elastic electron scattering", Phys. Rev., C 79, 44313\_1-44313\_7, 2009.

- [9] Antonov A. N., Hodgson P. E. and Petkov I. Z. "Nucleon momentum and density distribution in nuclei", Clarendon, Oxford, 1-165, 1988.
- [10] Antonov A. N., Nikolaev V.A., and Petkov I. Z. "Nucleon momentum and density distributions of nuclei", Z. Physik, A297, 257-260, 1980.
- [11] Antonov A. N., Hodgson P. E. and Petkov I. Z., *Nucleon correlation in nuclei* Springer-Verlag, Berlin-Heidelberg-New York, 1993.
- [12] Vries H. D., Jager C.W., and Vries C. "Nuclear Charge density distribution parameters from elastic electron scattering", Atomic data and nuclear data tables, 36 (3), 495-536, 1987.
- [13] Reuter W., Fricke G., Merle K. and Miska H. "Nuclear charge distribution and rms radius of  $^{12}\text{C}$  from absolute elastic electron scattering measurements", Phys. Rev. C 26, 806-818, 1982.
- [14] Hamoudi A. K., Hasan M. A. and Ridha A. R. "Nucleon momentum distributions and elastic electron scattering form factors for some 1p-shell nuclei", *Pramana Journal of Physics* (Indian Academy of Sciences), 78, (5), 737-748, 2012.
- [15] Hamoudi A. K., Flaiyh G. N. and Mohsin S. H. "Nucleon Momentum Distributions and Elastic Electron Scattering Form Factors for some sd-shell Nuclei", *Iraqi Journal of Science*, 53 (4), 819-826, 2012.
- [16] Hamoudi A. K. and Ojaimi H. F. "Nucleon momentum distributions and elastic electron scattering form factors for  $^{58}\text{Ni}$ ,  $^{60}\text{Ni}$ ,  $^{62}\text{Ni}$ , and  $^{64}\text{Ni}$  isotopes using the framework of coherent fluctuation model", *Iraqi Journal of Physics*, 12 (24), 33-42, 2014.
- [17] Hamoudi A. K., "Nucleon Momentum Distributions and Elastic Electron Scattering Form Factors for some sd-shell Nuclei", *Journal of Al-Nahrain University* 13 (2), 105-113, 2010.
- [18] Moustakidis C. C. and Massen S. E. "One-body density matrix and momentum distribution in s-p and s-d shell nuclei", Phys. Rev. C 62, pp: 34318\_1-34318\_7, 2000.
- [19] Traini M. and Orlandini G. "Nucleon momentum distributions in doubly closed shell nuclei", Z. Physik, A 321, pp: 479-484, 1985.
- [20] M. D. Ri, Stringari S. and Bohigas O. "Effects of short range correlations on one- and two-body properties of nuclei", Nucl. Phys. A 376, 81-93, 1982.

### الخلاصة

تم حساب توزيعات زخم النيكلون (NMD) للحالة الارضية وعوامل التشكل للاستطارة الالكترونية المرنة لبعض النوى الواقعة ضمن القشرة النووية  $1f-2p$  مثل نظائر الحديد  $^{54}\text{Fe}$ ،  $^{56}\text{Fe}$  و  $^{58}\text{Fe}$  وفقا ل نموذج تموج الكثافة المترابط الذي يعبر عنه بدلالة دالة التموج  $(|f(x)|^2)$ . لقد تم التعبير عن دالة التموج بدلالة توزيعات كثافة النيكلون وتم حسابها من النتائج النظرية والعملية. تميزت نتائج توزيعات زخم النيكلون (المستندة على دالة التموج النظرية والعملية) بخاصية الذيل الطويل عند قيم الزخوم العالية. أظهرت هذه الدراسة بان النتائج النظرية لعوامل التشكل للاستطارة الالكترونية المرنة لنظائر الحديد  $^{54}\text{Fe}$ ،  $^{56}\text{Fe}$  و  $^{58}\text{Fe}$  والمحسوبة بأنموذج التموج المتشابه تتفق مع النتائج العملية ولكل قيم الزخم المنتقل.